Instability mechanism in helicon-wave propagation in layered structures

Manvir S. Kushwaha
Department of Physics, Banaras Hindu University, Varanasi-221005, India
(Received 10 June 1985)

The surface-wave instability mechanism in the helicon-wave propagation in sandwich structures made up of n-type (IV-VI compound) semiconductors with anisotropic energy bands is investigated. The simplest geometry with magnetostatic field $\mathbf{B}_0||[100]||\hat{\mathbf{x}}$ is considered. The field solutions for unbounded media are obtained and thereafter the dispersion relation in the limit of $\omega_c\tau\rightarrow\infty$ is derived using the boundary conditions for the sandwich structure, which is further extended for the multilayered structures. The effect of collisions is also incorporated treating $\omega_c\tau$ large but finite. It is observed that the imaginary part of the dispersion relation which concerns the instability mechanism embodies a factor (D'), which accounts for the anisotropy of the effective masses of the charge carriers in the present system. The existence of D' results in reducing the dielectric mismatch (M) and hence the threshold velocity which triggers the instability. Since the instability part due to the surface wave is inversely proportional to M, the effect of D' increases the growth of the wave (above threshold velocity) and hence maximizes the efficiency of the multilayered structure as an amplifying device.

I. INTRODUCTION

Since they were predicted, the weakly damped, circularly polarized, transverse electromagnetic waves known as helicons (helicon waves) have been the most thoroughly studied of all the solid-state plasma waves.[1] The extensive investigations can be attributed to the fact that the helicon wave offers the opportunity for diagnosis of various parameters and properties of the crystalline solids through which it propagates. The device potential of helicon waves, as explored and argued by some scientists, has enhanced a considerable research interest in their own group in particular and many other research groups in general. Because the phase velocity of the helicon waves can be made significantly smaller than the speed of light, the idea of their amplification has attracted a lot of attention. The major practical interest in the solid-state plasma instabilities is the possibility of choosing physical conditions and adjusting geometries to maximize their growth rate and obtain from the solid-state plasma system the desired spectral distribution of high-frequency waves.

The first and the most noteworthy amplification scheme for helicon waves was put forth by Bok and Nozières.[2] They pointed out that the helicon wave can be unstable only when there are two types of charge carriers (of unequal densities) made to drift relative to each other. Notwithstanding the fact that numerous instabilities can be induced by drift velocities exceeding the phase velocity of the helicon wave, the detailed scheme proposed by Bok and Nozières[2] was criticized by some authors.[3–5] Subsequently, Baraff and Buchsbaum[6] (hereafter referred to as BB) suggested a novel instability mechanism utilized to amplify the helicon wave in only one-component-bounded solid-state plasmas. The noticeable feature of said mechanism is that the drift velocity needed to manifest the instability can be much smaller than the phase velocity of the wave. The lower drift velocity unquestionably avoids the risk of the heat dissipation effects associated with the large drift currents in the solids. For a good summary of the instability mechanism of BB, the reader is referred to Ref. 7.

The pioneering work of Baraff and co-workers[7–9] stimulated a lot of research interest in the surface-wave instability in helicon-wave propagation in layered structures.[10–12] The investigation of surface polaritons,[13] which are low-frequency electromagnetic modes localized at the free surfaces of the crystals (or at the interfaces in a composite structure), is of fairly recent vintage. Though the propagation of the bulk (helicon) wave in the Faraday geometry (when the magnetostatic field is parallel to the direction of propagation) and in the oblique geometry (when the magnetostatic field is inclined at an angle θ with the direction of propagation) is undisputed,[14] the possibility of the existence of low-frequency surface waves in the oblique geometry has been questioned by some authors.[13] This controversy has very recently been resolved by the present author,[15] particularly in the case of the layered structures. The instability mechanism of BB was reinvestigated[15] in the oblique-wave propagation, and the effective-mass ratio of charge carriers (electrons and holes) was incorporated. It was concluded that since the propagation of a bulk wave is permissible in the oblique geometry,[14] although for fairly small values of θ, so that the conditions of the helical regime are not violated, excitation of the surface wave which acts as a means to amplify the helicon wave in the same geometry is quite unquestionable.

The aforementioned references have all dealt with layered structures made up of the semiconductors whose Fermi surface is spherically symmetric and, hence, the effective mass of the charge carriers is a scalar quantity. The present investigation is aimed at studying the instability mechanism in the helicon-wave propagation in the layered structures made up of polar (PbX, $X\equiv$S,Se,Te) semicon-

ductors with anisotropic energy bands which have the ellipsoidal Fermi surface along the lines of BB. The effective mass of the charge carriers in the polar semiconductors is an anisotropic property and is therefore treated as a tensor quantity. The relevant physics of the polar semiconductors, of interest to a solid-state plasma physicist, has been briefly described in Sec. II. The motivation behind the choice of polar (PbX) semiconductors comprising the plasma media in the layered structures is twofold: (i) their technological importance, and (ii) the exotic, and possibly unique, characteristics exhibited by them.

The plan of this paper is as follows: In Sec. II is described the basic physics of the polar (PbX) semiconductors. In Sec. III we give most of the physics, relevant mathematics, and nearly all the approximations needed to calculate the dispersion relation for a sandwich structure with metalized surfaces (Fig. 1). We extend this dispersion relation for a multilayered structure (Fig. 2) and make a detailed diagnosis, discussing the instability mechanism in the existing system in Sec. IV. Section V is devoted to the conclusion drawn from our analytical treatment and the discussion of the merits of using PbX-type semiconductors as the plasma media in the layered structures. Our findings lend support to a preference for the polar (PbX) semiconductors over the nonpolar (II-VI and III-V compound) semiconductors to construct the semiconductor device used as an amplifier.

II. POLAR (IV-VI COMPOUND) SEMICONDUCTORS

The IV-VI compounds, PbS, PbSe, PbTe, and PbPo, often referred to collectively as the lead sulfide group of lead salts or lead-salt semiconductors, crystallize in the rocksalt (NaCl) structure.[16] The fundamental space lattice is the face-centered cubic; the reciprocal lattice is the body-centered cubic; the first Brillouin zone (BZ) is a truncated octahedron.[17] The interatomic bonds in these crystals are predominantly ionic in character and the lead salts are, therefore, also known as the polar semiconductors. Their ionicity f_i is expected to be larger than the critical ionicity f_c ($=0.785$) (Ref. 18) which distinguishes the more covalent fourfold-coordinated crystals (zinc-blende and wurtzite structures) with an ionicity $f_i < f_c$ from the more ionic sixfold-coordinated crystals (NaCl and CsCl structures) having an ionicity $f_i > f_c$. The crystal dynamics of the polar (PbS and PbTe) semiconductors[16] reveals that the frequency ω of the transverse optical (TO) phonons of the dispersion relation decreases sharply as the wave vector $\mathbf{k}$ approaches the zone center Γ. Thus the phonon energies $\hbar\omega$ for the lead salts are considerably smaller than the corresponding energies for the II-VI and III-V compound semiconductors. Consequently, the values of the static dielectric constant ϵ_0 for these crystals, calculated by using the Lyddane-Sach-Teller relation

$$[\epsilon_0/\epsilon_\infty = \omega_{\mathrm{LO}}^2(\Gamma)/\omega_{\mathrm{TO}}^2(\Gamma)] ,$$

are much larger than the values of ϵ_0 for II-VI and III-V compound semiconductors.

All the first three polar semiconductors (PbPo is less investigated and differs a little bit from this class) have a Fermi surface which consists of the prolate spheroids with the major axis along the [111] symmetry direction and the center lying at the L point in the first BZ. Within the first BZ, there are eight half-spheroids or, equivalently, four complete spheroidal constant-energy surfaces. The equation for these surfaces of constant energy E is

$$E = \frac{\hbar^2}{2}\left[\frac{k_1^2}{m_1} + \frac{k_2^2}{m_t} + \frac{k_3^2}{m_t}\right] ,$$

where k_1 is the component of the wave vector along the major axis of the spheroid and k_2 and k_3 are the components of the wave vector which are mutually orthogonal and lie in a plane perpendicular to k_1. m_1 and m_t are the longitudinal and transverse effective masses associated with the surface of constant energy. The spheroidal (or commonly the ellipsoidal) surfaces defined by the aforesaid equation are a good approximation to the Fermi surface of these crystals for low concentration, i.e., for the wave vectors near the band edges. For higher concentration and hence $\mathbf{k}$ values lying away from the band edges, there is a transition from an ellipsoidal Fermi surface (at lower concentrations) to a cylindrical Fermi surface as the concentration increases.

Since the topology of the Fermi surface specifies the behavior of the conduction electrons, a great qualitative difference is expected in the behavior of the semiconductors with a spherically symmetric Fermi surface (e.g., InSb) and those with an ellipsoidal Fermi surface (PbX). This difference is not, however, strictly due to the difference in the shape of the Fermi surfaces of the two types of semiconductors, but due rather to the tilt of the axis of the spheroid with respect to the magnetic field. When the magnetic field is tilted with respect to the axis of the spheroid, the effective-mass tensor has nonzero off-diagonal elements. In the PbX-type semiconductors, for an arbitrary magnetic field direction, a plane normal to the field would intersect each spheroid in a different way, the system being analogous to a gas of four different types of electrons, each type having a different effective mass.[19] The highly symmetric magnetic field configurations with magnetic field oriented along either the [100] or [110] directions are generally considered. In the former case, a plane perpendicular to the magnetic field cuts all the spheroids in an identical manner, indicating the same effective mass for the electrons in each of the four spheroids. Nevertheless, the behavior of the PbX-type semiconductors is different from that of the InSb-type semiconductors, owing to the difference in the shape of the Fermi surfaces. In the latter case, i.e., when the magnetic field is in the [110] direction, planes perpendicular to the field intersect each of two spheroids in an identical manner, implying effectively the presence of two types of electrons, each type having a different effective mass. The latter is expected to be a relatively complicated configuration as compared to the former.

A great deal of effort devoted to research activity in the polar (PbX) semiconductors can be attributed, in part, to the technological importance of these materials as detectors of infrared radiation. These PbX-type semiconductors exhibit some unusual, and possibly unique, properties

which stimulate additional research interest in these solids (viz., the following. The temperature coefficient dE_0/dT of the minimum energy gap E_0 is positive for PbS, PbSe, PbTe, whereas all the elemental or binary compounds exhibit negative values of dE_0/dT. The second anomalous property of the PbX group is defined as follows. It is well known that E_0 of a compound semiconductor MX is observed to decrease as the atomic number of atom X increases. This is a widely verified result for a large number of semiconductors. But the PbX group provides an exception to this, in that E_0 for PbSe is smaller than E_0 for PbTe. Thirdly, the static dielectric constants of the PbX group is unusually large compared to the values observed for the other semiconductors.)

III. FIELD SOLUTIONS AND DISPERSION RELATION

The sandwich structure depicted in Fig. 1 is assumed to be infinite in the x and z directions. The magnetostatic field $\mathbf{B}_0$ is taken to be parallel to the $[100]||\hat{\mathbf{x}}$ direction. The Maxwell-Boltzman transport equation governing the motion of electrons in the [111] spheroid is

$$\vec{\mathfrak{m}}\cdot(\dot{\mathbf{V}}+\mathbf{V}\cdot\nabla\mathbf{V}+\nu\mathbf{V})=q\left[\mathbf{E}+\frac{1}{c}\mathbf{V}\times\mathbf{B}\right], \tag{1}$$

where the symbols have their usual meanings.[15] The symbol $\vec{\mathfrak{m}}$ stands for the mass tensor which is a 3×3 matrix with nonvanishing off-diagonal elements. Equation (1) is linearized by taking $\mathbf{V}=\mathbf{V}_0+\mathbf{v}$, $\mathbf{E}=\mathbf{E}_0+\mathbf{e}$ and $\mathbf{B}=\mathbf{B}_0+\mathbf{b}$, where the terms on the right-hand sides of these expressions with (without) subscript zero are the dc (ac) parts of the respective quantities. Using $q\mathbf{E}_0=\vec{\mathfrak{m}}\cdot\mathbf{V}_0\nu$, Maxwell's curl field equation $\nabla\times\mathbf{e}=(1/c)\dot{\mathbf{b}}$ and spatial and temporal field dependence of the form $\sim e^{i(\mathbf{k}\cdot\mathbf{r}-\omega t)}$, we get from Eq. (1),

$$\zeta\frac{\vec{\mathfrak{m}}}{m_t}\cdot\mathbf{v}+i\boldsymbol{\beta}\times\mathbf{v}=-a^2\frac{\omega}{i4\pi N_0 q}[\mathbf{e}+\mathbf{U}\times(\mathbf{n}\times\mathbf{e})], \tag{2}$$

where

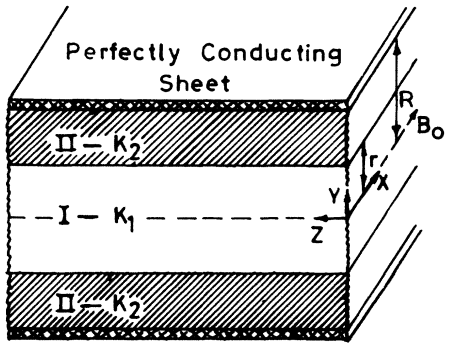

FIG. 1. Sandwich structure analyzed in the present treatment. Polar semiconductor plasma media I and II contain different carrier concentrations leading to different dielectric constants K_1 and K_2.

$$\zeta=1-\mathbf{n}\cdot\mathbf{U}+i\gamma,\quad a^2=\omega_p^2/\omega^2=\frac{4\pi N_0 q^2}{m_t\omega^2}, \tag{3}$$
$$\boldsymbol{\beta}=\omega_c/\omega=q\mathbf{B}_0/m_t c\omega,\quad \gamma=\nu/\omega,\quad \mathbf{U}=\mathbf{V}_0/c,\quad \mathbf{n}=c\mathbf{k}/\omega .$$

The index-of-refraction vector $\mathbf{n}$ is not to be confused with the scalar n emerging when we write density $N=N_0+n$.

In the existing configuration with $\mathbf{B}_0||[100]||\hat{\mathbf{x}}$, though the plane perpendicular to the magnetic field cuts all the spheroids in an identical manner, implying the same effective masses for electrons in each of the spheroids, the anisotropy of the effective masses of the charge carriers still prevails for the reasons explained in Sec. II. In order to account for this rather quasi-anisotropy of the effective masses of the charge carriers in the present configuration, we approximate the term $\vec{\mathfrak{m}}\cdot\mathbf{v}$ such that[20]

$$\vec{\mathfrak{m}}\cdot\mathbf{v}=m_{11}v_x\hat{\mathbf{x}}+m_{12}v_y\hat{\mathbf{y}}+m_{13}v_z\hat{\mathbf{z}},$$

where

$$m_{ij}=\frac{K_m+3\delta_{ij}-1}{3}m_t,$$

where δ_{ij} is the Kronecker delta, $K_m=m_1/m_t$. The solution of Eq. (2) can be expressed as follows:

$$\frac{i4\pi N_0 q}{\omega}\mathbf{v}=\frac{a^2/\zeta_1}{\beta^2-\zeta_2^2}\begin{bmatrix}\zeta_2^2-\beta^2 & 0 & 0\\ 0 & \zeta_1\zeta_2 & i\beta\zeta_1\\ 0 & -i\beta\zeta_1 & \zeta_1\zeta_2\end{bmatrix}\begin{bmatrix}1 & 0 & 0\\ Un_y & 1-Un_x & 0\\ 0 & 0 & 1-Un_x\end{bmatrix}\cdot\mathbf{e}, \tag{4}$$

where $u=|\mathbf{U}|$, $\beta=|\boldsymbol{\beta}|$, and ζ_1 and ζ_2 are, respectively, substituted for $\zeta(K_m+2)/3$ and $\zeta(K_m-1)/3$ for brevity. In obtaining Eq. (3) we have used the fact that $\mathbf{U}$ and $\boldsymbol{\beta}$ are parallel to $\hat{\mathbf{x}}$ and that n has no z component. Thus we have restricted our solution to be independent of z. Using the equation of continuity

$$\nabla\cdot\mathbf{g}+\dot{n}=0, \tag{5}$$

where $\mathbf{g}\ (=N_0\mathbf{v}+n\mathbf{V}_0)$ is the first-order part of the particle current $\mathbf{G}\ (=N\mathbf{V})$, we obtain

$$\mathbf{g}=N_0\left[\mathbf{v}+\frac{\mathbf{U}(\mathbf{n}\cdot\mathbf{v})}{1-Un_x}\right]. \tag{6}$$

The electric current $\mathbf{J}\ (=q\mathbf{g})$ now comes out to be

$$\mathbf{J}=N_0 q\begin{bmatrix}1/(1-Un_x) & Un_y/(1-Un_x) & 0\\ 0 & 1 & 0\\ 0 & 0 & 1\end{bmatrix}\cdot\mathbf{v}. \tag{7}$$

The correlation of Eqs. (4) and (7) gives

$$\left[\frac{4\pi i}{\omega}\right]\mathbf{J}=\overleftrightarrow{\mathscr{F}}\cdot\mathbf{e}\ , \tag{8}$$

where

$$\overleftrightarrow{\mathscr{F}}=\frac{a^2\beta}{\beta^2-\xi_2^2}\begin{bmatrix}\frac{1}{A\xi_1\beta}(\xi_2^2-\beta^2+\xi_1\xi_2B^2) & \frac{1}{\beta}\xi_2B & iB\\ \frac{1}{\beta}\xi_2B & \frac{1}{\beta}\xi_2A & iA\\ -iB & -iA & \frac{1}{\beta}\xi_2A\end{bmatrix},$$

where $A=1-Un_x$ and $B=Un_y$. The current expressed in Eq. (8) acts as a source of the magnetic field $\mathbf{b}$ via Maxwell's fourth curl field equation

$$\nabla\times\mathbf{b}=\frac{4\pi}{c}\mathbf{J}+\frac{1}{c}\dot{\mathbf{e}}\ . \tag{9}$$

Using Maxwell's third curl field equation

$$\mathbf{b}=\frac{c}{i\omega}(\nabla\times\mathbf{e}) \tag{10}$$

to eliminate $\mathbf{b}$ in Eq. (9) and using Eq. (8), gives us

$$\overleftrightarrow{\mathscr{K}}\cdot\mathbf{e}+\mathbf{n}\times(\mathbf{n}\times\mathbf{e})=0 \tag{11}$$

where

$$\overleftrightarrow{\mathscr{K}}=\overleftrightarrow{\mathbf{1}}+\overleftrightarrow{\mathscr{F}}\ . \tag{12}$$

In order to simplify the analysis, we further invoke the helicon approximation[6] in Eqs. (11) and (12), which leaves us with

$$\zeta_i=iD_i\gamma=iD_i/\omega\tau\ , \tag{13}$$

with the assumption that $\gamma\gg1$ and that even at largest drift current Un_x will be of the order of unity. The subscript $i=1$ and 2, respectively, refers to D_1 $[=(K_m+2)/3]$ and D_2 $[=(K_m-1)/3]$. The ratio ζ_i/β becomes

$$\zeta_i/\beta=iD_i/\omega_c\tau\ . \tag{14}$$

Assuming $\omega_c\tau\gg1$ and retaining the term of the order of $1/\omega_c\tau$ gives

$$a^2\beta/(\beta^2-\xi_2^2)\approx a^2/\beta=\frac{\omega_p^2}{\omega_c\omega}\equiv K\ . \tag{15}$$

Further, the unit tensor $\overleftrightarrow{\mathbf{1}}$ is neglected from Eq. (12) in the helicon approximation. This is, in a way, equivalent to the neglect of the displacement current in a dense (solid-state) plasma. Using Eqs. (13), (14), and (15) in Eq. (11), determining the electric field, gives us

$$\begin{bmatrix}P+Qn_y^2 & (iZ+n_x)n_y & iYn_y\\ (iZ+n_x)n_y & S-n_x^2 & iX\\ -iYn_y & -iX & S-n_x^2-n_y^2\end{bmatrix}\begin{bmatrix}e_x\\ e_y\\ e_z\end{bmatrix}, \tag{16}$$

where

$$X=KA,\quad Y=KU,\quad Z=\frac{KD_2U}{\omega_c\tau}\ ,$$
$$P=\frac{iK\omega_c\tau}{AD_1},\quad S=\frac{iKD_2A}{\omega_c\tau},\quad Q=\frac{iKD_2U^2}{A\omega_c\tau}-1\ . \tag{17}$$

The nontrivial solution of Eq. (16) gives a quadratic equation in n_y^2 such that

$$an_y^4+bn_y^2+c=0\ , \tag{18}$$

where a, b, and c in terms of X, Y, Z, P, Q, and S, as defined in Eq. (17), in the present analysis, come out in exactly the same forms as expressed by BB [their Eq. (2.15)], with their n_z replaced by n_x.

The calculation of the transverse field components e_y and e_z in terms of the tangential field component e_x gives

$$De_z=in_y[Y(S-n_x^2)-iX(Z-in_x)]e_x\ , \tag{19a}$$
$$De_y=-in_y[(S-n_x^2-n_y^2)(Z-in_x)+iXY]e_x\ , \tag{19b}$$
$$D=[S^2-S(2n_x^2+n_y^2)+n_x^2(n_x^2+n_y^2)-X^2]\ , \tag{19c}$$

from Eq. (16). It is observed, from Eq. (17), that the following relations, which would be helpful to simplify the analysis, hold well:

$$(X+n_xY)^2\equiv K^2=-PSD' \tag{20a}$$

and

$$SY=iXZ\ , \tag{20b}$$

where $D'=D_2/D_1$. Expanding a, b, and c in terms of the inverse power of $\omega_c\tau$, retaining the lowest-order terms in $(\omega_c\tau)^{-1}$, and treating $\omega_c\tau\gg1$, leaves us with

$$a=S+i2n_xZ+(Q+1)n_x^2=iKD_2/A\omega_c\tau\ , \tag{21a}$$
$$b=Pn_x^2\ , \tag{21b}$$
$$c=P(n_x^2-X^2)\ . \tag{21c}$$

The algebraic solution of Eq. (18), expressible as

$$n_y^2=\frac{1}{2a}[-b\pm(b^2-4ac)^{1/2}]\ ,$$

now gives, in the lowest-order terms, $n_y^2=-c/b$ and $n_y^2=-b/a$. In the second solution we substitute $N_y=in_y$ so that the two roots are

$$n_y^2=-\frac{c}{b}=\frac{X^2}{n_x^2}-n_x^2\ , \tag{22a}$$
$$N_y^2=+\frac{b}{a}=\frac{n_x^2}{D_1D_2}(\omega_c\tau)^2\ . \tag{22b}$$

We will hereafter designate electric field components in Eqs. (19) by the superscript b (for bulk wave) and s (for surface wave) corresponding to the solutions in (22a) and (22b), respectively. Making use of Eqs. (20) in Eqs. (19) and retaining the terms of the lowest order in $(\omega_c\tau)^{-1}$, results in substituting Eqs. (22) in Eqs. (19) to give

TABLE I. Solution types. A zero indicates that the entry is one order of $\omega_c\tau$ smaller than the other entries in the same row.

Type j	e_x	e_z	b_x	b_z
$j=1$	0	$E_z^1\sin(ky)$	$B_x^1\cos(ky)$	$B_z^1\sin(ky)$
$j=2$	$E_x^2\cosh(Ky)$	0	$B_x^2\cosh(Ky)$	$B_z^2\sinh(Ky)$
$j=3$	0	$E_z^3\cos(ky)$	$B_x^3\sin(ky)$	$B_z^3\cos(ky)$
$j=4$	$E_x^4\sinh(Ky)$	0	$B_x^4\sinh(Ky)$	$B_z^4\cosh(Ky)$
$j=5$	$E_x^5e^{Ky}$	0	$B_x^5e^{Ky}$	$B_z^5e^{Ky}$
$j=6$	$E_x^6e^{Ky}$	0	$B_x^6e^{-Ky}$	$B_z^6e^{-Ky}$

$$D^b e_z^b=(-in_y n_x K)e_x^b\ , \tag{23a}$$

$$D^b e_y^b=(n_y XK/n_x)e_x^b\ , \tag{23b}$$

$$D^b=Sn_y^2D'\ , \tag{23c}$$

and

$$D^s e_z^s=(-N_y n_x K)e_x^s\ , \tag{24a}$$

$$D^s e_y^s=(iN_y^3 n_x)e_x^s\ , \tag{24b}$$

$$D^s=-N_y^2 n_x^2\ . \tag{24c}$$

The corresponding magnetic field components, using $\mathbf{b}=\mathbf{n}\times\mathbf{e}$, come out as

$$b_x^b=(-in_x K/SD')e_x^b\ , \tag{25a}$$

$$b_y^b=(in_x^2 K/SD'n_y)e_x^b\ , \tag{25b}$$

$$b_z^b=(XK/SD'n_y)e_x^b\ , \tag{25c}$$

and

$$b_x^s=(-iK/n_x)e_x^s\ , \tag{26a}$$

$$b_y^s=(-K/N_y)e_x^s\ , \tag{26b}$$

$$b_z^s=[-iN_y(S+in_x Z)/n_x^2]e_x^s\ . \tag{26c}$$

It is worth mentioning that K and X in the analysis served, respectively, as the dielectric constant and the effective (Doppler-shifted) dielectric constant. There are four tangential field components e_x, e_z, b_x, and b_z in each (bulk and surface-wave) solution. In type-b solutions, e_x^b is one order of $\omega_c\tau$ smaller than the other three field components. In type s, on the other hand, e_z^s is one order of $\omega_c\tau$ smaller than the other three field components. When the boundary conditions are set up, equating these two small components to zero not only simplifies the complexity but also still renders the results correct to lowest order in $1/\omega_c\tau$.[6] Following BB (see the last paragraph in Sec. II of Ref. 6), the solution types in the existing system are exhibited in Tables I and II in which we have denoted k for $\omega n_y/c$ and K for $\omega N_y/c$.

In regions I and II (Fig. 1) the actual fields will be the sums of the solutions listed in Tables I and II, each solution in the sum being multiplied by an arbitrary constant. These arbitrary constants must be adjusted such that (see Table III in Ref. 6) the boundary conditions[6] are satisfied. Following Appendix A in Ref. 6, we obtain the following dispersion relation:

$$n_2\cot[k_2(r-R)]=n_1\cot\left[k_1 r+\eta\frac{\pi}{2}\right]-i\frac{(K_1-K_2)(X_1-X_2)}{\sqrt{D'}n_x(K_1+K_2)}\ , \tag{27}$$

where

$$X_i=K_i(1-U_i n_x)\ , \tag{28a}$$

$$k_i=\omega n_i/c\ , \tag{28b}$$

$$n_i^2=X_i^2/n_x^2-n_x^2\ , \tag{28c}$$

where the subscript $i=1(2)$ refers to the respective quantities in regions I (II) of the sandwich structure (Fig. 1). $\eta=0$ for the even modes and 1 for the odd modes. The classification of the modes is designated as even or odd depending on whether $b_x(y)=\pm b_x(-y)$. In the odd mode $b_x(y)=-b_x(-y)$ and in the even mode $b_x(y)=+b_x(-y)$. The comparison of Eq. (27) and Eq. (3.1) in Ref. 6 reveals a difference of factor D' which accounts for the effective-mass anisotropy of the charge carriers in the present system.

IV. DIAGNOSIS OF DISPERSION RELATION

The diagnosis of real and imaginary parts in the dispersion relation, Eq. (27), for the normalized drift velocity U near threshold (drift) velocity U^0 is of considerable im-

TABLE II. Solution constants.

Type j	E_x	E_z	B_x/i	B_z/i
$j=1$		$n_x K/Sn_y D'$	$-n_x K/SD'$	$XK/Sn_y D'$
$j=2$	1		$-K/n_x$	$-Ny(S+in_x Z)/n_x^2$
$j=3$		$n_x K/Sn_y D'$	$+n_x K/SD'$	$XK/Sn_y D'$
$j=4$	1		$-K/n_x$	$-N_y(S+in_x Z)/n_x^2$
$j=5$	1		$-K/n_x$	$-N_y(S+in_x Z)/n_x^2$
$j=6$	1		$-K/n_x$	$+N_y(S+in_x Z)/n_x^2$

portance. At threshold velocity the wave changes from decaying to growing and hence the propagation constant n_x becomes purely real. As a result, the imaginary part of Eq. (27) must vanish. This can happen if $K_1=K_2$ or $X_1=X_2$. The latter choice is, however, preferred since the former always gives a real n_x for all values of U. This then leads us to $X_1=X_2$, or

$$K_1(1-U_1^0 n_x^0)=K_2(1-U_2^0 n_x^0) . \tag{29}$$

Equation (29) yields $n_1=n_2$ ($=n_0$, say) and $k_1=k_2$ ($=k_0$, say). Then from Eq. (27) we have

$$\cot[k_0(r-R)]=\cot\left[k_0 r+\eta\frac{\pi}{2}\right] ,$$

which gives

$$k_0\left[=\frac{\omega n_0}{c}\right]=\frac{m\pi}{2R}, \quad m=1,2,3,\ldots . \tag{30}$$

Integer m in Eq. (30) is even for $\eta=0$ and odd for $\eta=1$. The condition (30) stating, that at threshold an integer multiple of transverse half-wavelength spans the full thickness of the sandwich structure, is clearly a consequence of equating X_1 to X_2. In other words, the wave propagates in the sandwich structure regardless of the interfaces or the difference of the media.

For the sake of simplicity, we assume that only the carriers in medium I drift, so that $U_2^0=0$ and the relation (29) still holds well. Then the threshold (drift) velocity U_t ($\equiv U_1^0$) is given by

$$U_t=\frac{1}{n_x^0}(1-K_2/K_1)=\frac{(\xi-1)}{n_x^0\xi} \tag{31a}$$

or

$$V_t=\frac{(\xi-1)}{\xi}V_\phi=-\frac{M}{\xi}V_\phi , \tag{31b}$$

where V_ϕ ($=c/n_x^0=\omega/\mathrm{Re}k_x$) is the phase velocity of the bulk wave and M ($=1-\xi$) is the so-called dielectric mismatch, ξ being defined as $\xi=K_1/K_2$. Having obtained k_0, one can solve, Eq. (28c) for n_x. Thus

$$\epsilon=\left[\frac{n_x^0}{(K_2)^{1/2}}\right]^2=\tfrac{1}{2}[(T^4+4)^{1/2}-T^2] , \tag{32a}$$

where

$$T=\frac{n_0}{(K_2)^{1/2}}=\frac{ck_0}{\omega(K_2)^{1/2}} . \tag{32b}$$

We now solve for n_x when U_1 is in the neighborhood of U_t. To do so, we expand all the quantities (U, n_x, n_1, n_2) in Eq. (27) to first order in U_1-U_t. For the details of the expansion, the reader is referred to Appendix B of Ref. 6. Writing

$$n_x=n_x^0+\gamma(U_1-U_t) , \tag{33}$$

a laborious algebraic manipulation gives us

$$\gamma=\frac{K_2(\cot\phi-k_0 r\csc^2\phi)+i\xi(1-\xi)n_x^0 n_0/\sqrt{D'}(1+\xi)}{k_0 R\csc^2\phi+(1-\xi)J} , \tag{34}$$

where

$$J=\left[\frac{1}{\epsilon}(\cot\phi-k_0 r\csc^2\phi)-i\xi U_t n_0/\sqrt{D'}(1+\xi)\right] ,$$

$$\alpha=\epsilon+1/\epsilon ,$$

and $\phi=k_0(r-R)$. Letting $\xi\to 1$, we obtain

$$\mathrm{Re}\gamma^{(2)}=-\frac{K_2}{\alpha}\frac{r}{R} \tag{35}$$

and

$$\mathrm{Im}\gamma^{(2)}=\frac{n_x^0(1-\xi)\sin^2\phi}{2\sqrt{D'}\alpha\omega R/c} . \tag{36}$$

The bracketed superscript denotes the number of interfaces in the structure. The text following Eq. (3.5) in Sec. III of Ref. 6 argues that Imγ will be half as large for a one-interface structure as for a two-interface structure. The expression for a one-interface structure of width $2R$ then follows by replacing R by $2R$ in Eqs. (30), (32), (35), and (36). Therefore, Eqs. (35) and (36) for a one-interface structure are

$$\mathrm{Re}\gamma^{(1)}=-\frac{K_2}{\alpha}\frac{r}{2R} , \tag{37}$$

$$\mathrm{Im}\gamma^{(1)}=\frac{n_x^0(1-\xi)\sin^2\phi}{4\sqrt{D'}\alpha\omega R/c} . \tag{38}$$

Now, we are interested in extending the analysis in the multilayered structures (MLS) (Fig. 2). In MLS of N unit cells the summation of Eq. (38) over the positions of all internal interfaces gives[8]

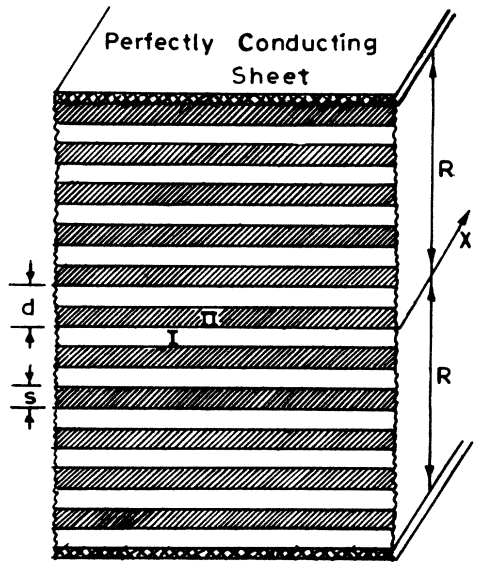

FIG. 2. Multilayered structure. A generalization of the sandwich structure (Fig. 1) with equal width s of each of the two semiconductor slabs. The system is periodic in the y direction (with period d) and infinite in the x and z directions.

$$\mathrm{Im}\gamma^{\mathrm{MLS}}=\frac{n_x^0(1-\xi)}{2\sqrt{D'}\alpha\omega d/c} . \tag{39}$$

Similarly, summing Eq. (37) over all the $2N-1$ internal interfaces in MLS gives, assuming $d_1=d_2=d/2$,

$$\mathrm{Re}\gamma^{\mathrm{MLS}}=-\frac{K_2}{\alpha} . \tag{40}$$

These calculations, in which the analysis in sandwich structure has been extended to MLS, are all performed in the limit of $\omega_c\tau\to\infty$. A study of $(\omega_c\tau)^{-1}$ correction would reveal the most important loss mechanism, i.e., the collisional loss (CL) of the bulk wave. The CL is an inherent characteristic of actual materials wherein the carriers always suffer some collisions and hence cannot, in principle, be ignored. To account for the CL, we seek a relationship between k_x, k_y, and ω (which exists because of Maxwell's equations and the transport equation for carriers), depending upon the plasma parameters characterizing the medium in which the wave exists. This relation, quite analogous to the one in footnote 7 of Ref. 6, in the present system becomes

$$n_y^2=\frac{X^2}{n_x^2-S(1+D')}-\frac{n_x^2(n_x^2-2S)}{n_x^2-S(1+D')} . \tag{41}$$

Considering Eq. (41) in medium II at threshold ($k_0=m\pi/2R$) gives

$$\left[\frac{m\pi c}{2\omega R}\right]^2=n_0^2=\frac{K_2^2}{n_x^2-S(1+D')}-\frac{n_x^2(n_x^2-2S)}{n_x^2-S(1+D')} , \tag{42}$$

with $S=iK_2D_2/\omega_c\tau$ for medium II. To lowest order in $(\omega_c\tau)^{-1}$, Eq. (42) gives, using $n_x=n_x^0+\gamma p$, with $p=1/\omega_c\tau$,

$$\mathrm{Im}\gamma^{\mathrm{CL}}=\frac{1}{2}\frac{n_x^0}{(\epsilon+\epsilon^3)}[D''+\epsilon^2(2-D'')] \tag{43}$$

or

$$\mathrm{Im}n_x^{\mathrm{CL}}=(\omega_c\tau)^{-1}\mathrm{Im}\gamma^{\mathrm{CL}} , \tag{44}$$

where $D''=D_2(1+D')$. The expression (44) gives the value of $\mathrm{Im}n_x$ due to collisional losses in the bulk at the threshold, i.e., when the surface wave disappears. There is no reason to suspect that the situation will be any different in MLS, simply because the expression of $\mathrm{Im}n_x^{\mathrm{CL}}$ is independent of the position of the internal interfaces.

Since in MLS the gain or loss, depending upon the sign of $\mathrm{Im}n_x$, per interface is truly additive,[8] the total n_x from Eq. (33) becomes, using Eqs. (39) and (40) and adding the effect of collisions via Eq. (44),

$$n_x=n_x^0\left[1-\frac{K_2(U-U_t)}{n_x^0}+\frac{i}{\alpha}\left[\frac{(1-\xi)(U-U_t)}{\sqrt{D'}2\omega d/c}+\frac{(\omega_c\tau)^{-1}}{2\epsilon^2}F\right]\right] , \tag{45}$$

where F is substituted for $D''+\epsilon^2(2-D'')$ for brevity. It is useful for further analysis to write the dispersion relation, Eq. (45), in the form

$$k=\frac{2\pi}{\lambda_H}\left[1-\frac{(V-V_t)/V_H}{2\epsilon^{1/2}}+\frac{i}{\alpha}\left[\frac{(1-\xi)\omega_c\tau(V-V_t)/V_H}{\sqrt{D'}8\pi n_c}+\frac{(\omega_c\tau)^{-1}}{2\epsilon^2}F\right]\right] , \tag{46}$$

where, assuming the interfaces in MLS (Fig. 2) to be equally spaced ($s=d/2$), the symbols used in Eq. (46) are defined below:

$$n_c=s/\delta,\quad \delta=\lambda_H/\omega_c\tau,\quad \lambda_H=2\pi V_H/\omega,\quad V_H=c/(K_2)^{1/2} ,$$
$$V_t\,|_{\xi\to1}=V_\phi(\xi-1),\quad V_H=\epsilon^{1/2}V_\phi . \tag{47}$$

Though the terms defined in Eq. (47) have their usual conventional meanings, it would still be better to identify them: λ_H and V_H are, respectively, the helicon wavelength and helicon-wave velocity in medium II. δ is an e-fold distance with which the surface wave decays exponentially away from the interfaces. The separation s between the consecutive interfaces is assumed to be sufficiently large so that the surface wave excited at one interface does not extend to the next interface. On the other hand, s should be sufficiently small so that many interfaces can be fitted across the structure.

In the limit $\xi\to1$, V_t can be made smaller when V_ϕ is reduced. The appropriate choice[7] for lowering V_t is for the total width of the structure $2R\gtrsim\lambda_H$, i.e., when the helicon wavelength spans the full thickness of the structure. This choice gives, via Eqs. (42) and (32), $T=\frac{1}{2}$ leading to $\epsilon\approx\frac{7}{8}$, $\alpha\approx2$, and $F\approx2$, and further simplifies Eq. (46) to

$$k=\frac{2\pi}{\lambda_H}\left[1-\frac{(V-V_t)/V_H}{2}+i\left[\frac{(1-\xi)\omega_c\tau(V-V_t)/V_H}{\sqrt{D'}16\pi n_c}+\frac{1}{2\omega_c\tau}\right]\right] . \tag{48}$$

In order to judge the operating characteristics and efficiency of the device used as an amplifier, it seems desirable to analyze the dispersion relation, Eq. (48). The best value of ξ is that which gives the lowest possible threshold velocity V_{t0}, threshold being defined now by the requirement that the wave vector $\mathbf{k}$ be real (or, $\mathrm{Im}k=0$). This then gives

$$V_{t0}=-\left[\frac{(8\pi n_c\sqrt{D'})^{1/2}}{(\omega_c\tau)^2M}+M\right]V_H , \tag{49}$$

since $V_\phi\approx V_H$ if $\epsilon\approx1$. The optimum M that gives the lowest threshold velocity becomes

$$M=\pm\frac{(8\pi n_c\sqrt{D'})^{1/2}}{\omega_c\tau} \tag{50}$$

and, therefore, the corresponding actual threshold velocity is

$$V_{t0}=-2MV_H\approx-2MV_\phi . \tag{51}$$

Thus the propagation wave vector k in terms of the op-

timum M can be written as

$$k=\frac{2\pi}{\lambda_H}\left[1-\frac{1}{2}\left[\frac{V}{V_H}\pm\frac{(8\pi n_c\sqrt{D'})^{1/2}}{\omega_c\tau}\right]+i\left[\pm\frac{1}{2(8\pi n_c\sqrt{D'})^{1/2}}\frac{V}{V_H}+\frac{1}{\omega_c\tau}\right]\right]. \quad (52)$$

In Eq. (50) the factor D' which is always less than unity will reduce the dielectric mismatch M. The actual threshold velocity V_{t0} can, therefore, be made arbitrarily small by making the dielectric mismatch small. Since the imaginary part of k, in Eq. (52), is inversely proportional to M, the growth or decay of the wave (and hence power gain or loss at the interfaces) will be larger with the smaller value of M. In view of the existing form ($\sim e^{i\mathbf{k}\cdot\mathbf{r}}$) of the spatial dependence of the fields, the negative (positive) Imk will lead to the growth (decay) of the wave and hence power gain (loss) generated at the interfaces. Therefore, from Eq. (48) it is found that in the absence of the collisional losses, the wave will neither grow nor decay if $\xi=1$. It is the threshold condition which always gives real n_x (or k) for all values of the drift velocity (U). When $\xi<1$, the wave decays and hence M is positive [see Eq. (50)], a situation below the threshold condition. On the other hand, if $\xi>1$, M will be negative and the wave will grow. The latter is the condition arising due to the phase reversal of the surface wave (above threshold velocity) which gives rise to the instability. With the finite collisional losses, the condition for the growth rate (or power gain)

$$V/V_H \gg 2(8\pi n_c\sqrt{D'})^{1/2}/\omega_c\tau$$

has to be satisfied. Since the surface wave decays exponentially away from the interfaces with an e-fold distance δ, $n_c=s/\delta=2$ is probably an adequate compromise for practical purposes. As such, the value of M which in the helical regime ($\omega_c\tau\to\infty$ and $\omega\tau\gg1$) is always less than unity lends support to the fact that the actual threshold velocity sufficient to trigger the instability is much smaller than the phase velocity of the wave.

V. CONCLUSION

We have investigated the surface-wave instability mechanism in the helicon-wave propagation in the layered (sandwich and multilayered) structures wherein the PbX-type semiconductors form the plasma media. It is found that the factor D' which is always less than one and accounts for the anisotropy of the effective masses of the charge carriers plays a significant role in achieving the greater efficiency of the system at the smallest possible value of the threshold (drift) velocity. In solids with spherical Fermi surfaces (e.g., II-VI and III-V compound semiconductors) the factor $D'=1$, and the only option left for choosing the better material, is the plasma parameter $\omega_c\tau$—the larger the $\omega_c\tau$, the smaller that velocity will be. Therefore, the preference for the choice of IV-VI polar semiconductors over the II-VI and III-V ones, as the plasma media in the layered structures, gives us an additional advantage in increasing the growth of the wave (or power gain generated at the interfaces) and hence in maximizing the efficiency of the solid-state device used as an amplifier.

ACKNOWLEDGMENTS

The author takes pleasure in acknowledging stimulating discussions with Professor R. N. Singh. He is also grateful to Professor S. J. Buchsbaum and Professor G. A. Baraff for useful communication which aided in resolving some of the problems. I am thankful to Professor P. Halevi for drawing my attention to the utility of extending my work (Ref. 15) to the polar semiconductors. This work was supported by the University Grants Commission, New Delhi.

[1]M. Glicksman, Solid State Phys. **26**, 275 (1971); Adv. Plasma Phys. **5**, 261 (1974).
[2]J. Bok and P. Nozières, J. Phys. Chem. Solids **24**, 709 (1963).
[3]T. Misawa, Jpn. J. Appl. Phys. **2**, 500 (1963).
[4]A. Bers and A. L. McWhorter, Phys. Rev. Lett. **15**, 755 (1965).
[5]A. Hasegawa, J. Phys. Soc. Jpn. **20**, 1072 (1965).
[6]G. A. Baraff and S. J. Buchsbaum, Phys. Rev. **144**, 260 (1966).
[7]R. N. wallace and G. A. Baraff, J. Appl. Phys. **37**, 2937 (1966).
[8]L. M. Saunders and G. A. Baraff, J. Appl. Phys. **37**, 4551 (1966).
[9]G. A. Baraff, J. Phys. Chem. Solids **28**, 1037 (1967).
[10]R. Hirota, J. Phys. Soc. Jpn. **23**, 798 (1967).
[11]A. C. Baynham, A. D. Boardman, M. R. B. Dunsmore and J. Tierney, IEEE Trans. Micro Theory Tech. **21**, 111 (1973).
[12]N. N. Beletzky, Solid State Commun. **14**, 820 (1974).
[13]P. Halevi, in *Electromagnetic Surface Modes,* edited by A. D. Boardman (Willey, New York, 1982), p. 249.
[14]M. C. Steele and B. Vural, *Waves and Interactions in Solid State Plasmas,* (McGraw-Hill, New York, 1969); P. M. Platzman and P. A. Wolf, *Waves and Interactions in Solid State Plasmas,* Vol. 13 of *Solid State Physics,* edited by H. Ehrenreich, F. Seitz, and D. Turnbull (Academic, New York, 1973).
[15]M. S. Kushwaha, Solid State Electronics (to be published).
[16]R. Dalven, Solid State Phys. **28**, 179 (1973).
[17]M. S. Kushwaha, Ph.D. thesis, Banaras Hindu University, 1980.
[18]J. C. Phillips, Rev. Mod. Phys. **42**, 371 (1970).
[19]R. F. Wallis, in *Electromagnetic Surface modes,* Ref. 13, p. 575.
[20]Having gone through the complete analysis the way it is presented in the article and even otherwise (i.e., with $\tilde{m}$ being treated as the full 3×3 matrix), it was found that the present approximation not only avoids the mathematical complexity but also explicitly accounts for a better effective-mass anisotropy in the present field configuration in the existing system.